Supplementary Information

Constructing Ultramicropores Structures in Hard Carbon via Low-Temperature Force-Field-Induced Esterification Reactions for Enhancing Sodium Storage

Ning Zhang,[a] Zongfu Sun,[*a] Wen Li,[a] Nan Xiao,[a] Hui Xie,[a] Biao Chen,[a] Naiqin Zhao,[a] and Chunnian He[*abc]

[a] School of Materials Science and Engineering, National Industry-Education Platform of Energy Storage and Tianjin Key Laboratory of Composite and Functional Materials, Tianjin University, Tianjin 300350, P. R. China

[b] State Key Laboratory of Precious Metal Functional Materials, Tianjin University, Tianjin, 300350, P. R. China

[c] Joint School of National University of Singapore and Tianjin University, International Campus of Tianjin University, Fuzhou 350207, Fujian, P. R. China

Experimental

Materials synthesis

Firstly, the phenolic resin purchased from Henan Borun New Material Co. was annealed at 300 °C with a heating rate of 5 °C min^{-1} under an Ar atmosphere for 1h, obtaining the PHC product. Subsequently, the PHC was placed in a vacuum furnace, applied a pressure of 20 MPa, and carbonized under vacuum at 900 °C for 2 h with a heating rate of 5 °C min^{-1} to obtain HC-20. By changing the pressure to 10 and 30 MPa, the obtained samples are indicated as HC-10 and HC-30. As a control, HC-0 was prepared by direct carbonization of the PHC at 900 °C for 2 h under an Ar atmosphere with a heating rate of 5 °C min^{-1}.

Materials characterization

The microstructure of the samples was obtained by scanning electron microscope (SEM, S-4800) and high-resolution transmission electron microscopy (HR-TEM, JEM-2100F). Fourier transform infrared spectroscopy(FTIR) was performed on Bruker INVENIO S. The microcrystalline structure was analyzed using x-ray diffraction (XRD, Rigaku SmartLab) with Cu Kα radiation (λ=1.54056 Å) and Raman spectroscopy (Raman XploRA Plus) with a laser wavelength of 532 nm. The pore structure of the samples was characterized by N_2 and CO_2 adsorption/desorption isotherms on a Micromeritics ASAP 2460 analyzer. The small-angle X-ray scattering (SAXS) spectra were obtained using Xenocs Xeuss 2.0. The X-ray photoelectron spectroscopy (XPS) analysis was performed on a Kratos Axis Ultra DLD spectrometer.

Electrochemical characterization

The electrochemical performance of the samples was evaluated in CR2032 coin cells. The anode slurry was prepared from obtained hard carbon materials, carbon black (CB), and sodium alginate with the mass ratio of 8:1:1. The slurry was well mixed in ultrapure water, coated on copper foil, and dried at 80 °C for 12 h in a vacuum. The electrodes were punched into 12 mm diameter disks, and the active material loading was controlled in the range of 1.2-1.5 mg cm^{-2}. Sodium metal foil was employed as the counter electrode, and glass fiber was used as the separator. The commercial electrolyte of 1 mol L^{-1} $NaPF_6$ in diglyme was used. The cells were assembled in an argon-filled

glove box (O_2, H_2O < 0.1 ppm) and tested at a constant temperature of 25 °C. The galvanostatic charge-discharge (GCD) measurement and galvanostatic intermittent titration technique (GITT) were tested by the Neware battery test system with 0.001-2.5 V. The cyclic voltammetry (CV) measurements and electrochemical impedance spectroscopy (EIS) were performed on a CHI 660D Electrochemical Workstation.

The full cell was assembled with HC-20 as the anode and layered O_3-$NaNi_{1/3}Fe_{1/3}Mn_{1/3}O_2$ (NFM) as the cathode, and the N/P ratio of 1.2. Before assembly, the HC-20 was presodiated by cycling 3 times at a voltage window of 0.001-2.5 V, and the NFM was also cycled 3 times at 2-4 V. The GCD test of HC-20//NFM was performed at 25 mA g^{-1} under a voltage range of 2-4 V vs. Na^+/Na, with an electrolyte of 1 mol L^{-1} $NaPF_6$ in DMC/EC/EMC (2:1:2 by volume).

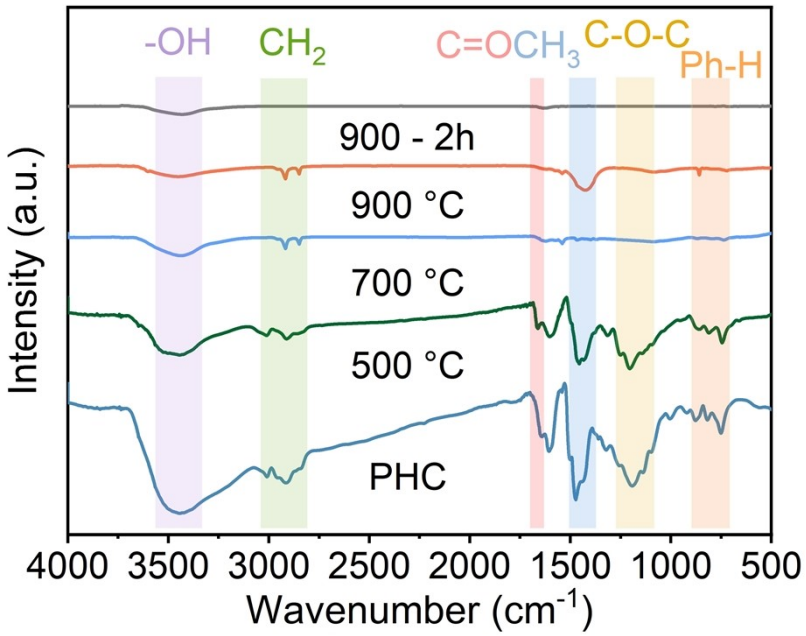

Fig. S1 *Ex situ* FTIR spectra of HC-0.

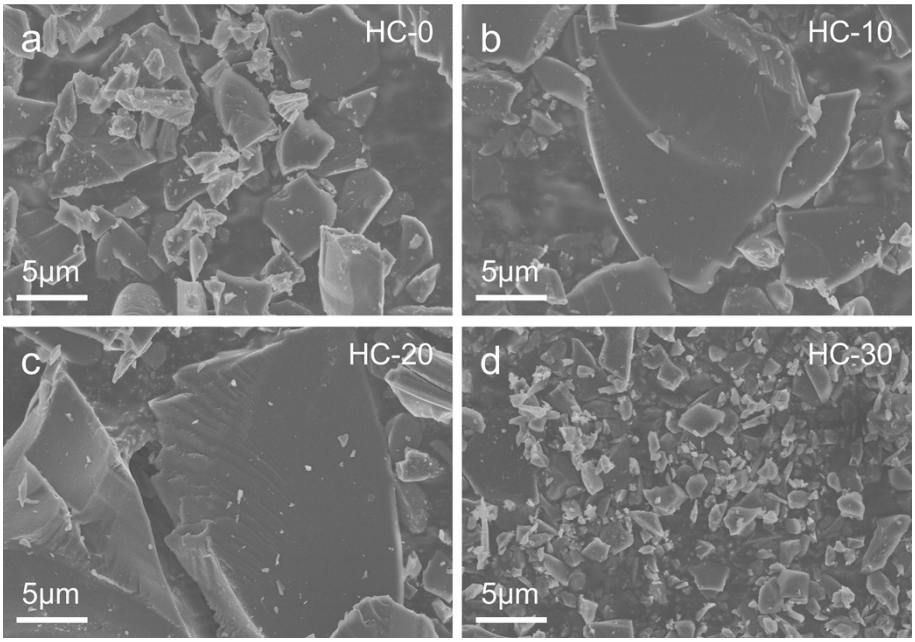

Fig. S2 SEM images of (a) HC-0, (b) HC-10, (c) HC-20, and (d) HC-30.

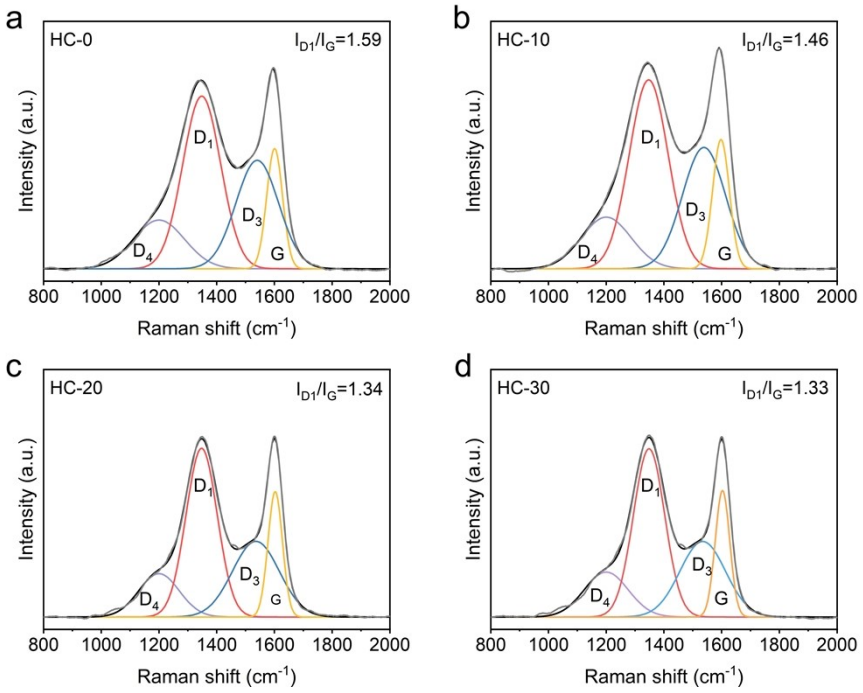

Fig. S3 Peak fitting of the Raman spectra: (a) HC-0, (b) HC-10, (c) HC-20, and (d) HC-30.

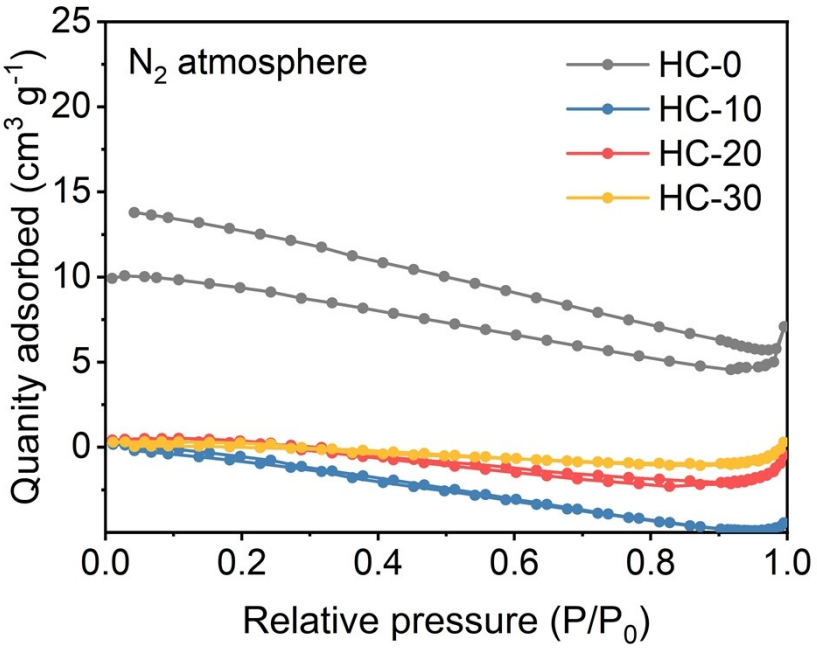

Fig. S4 N_2 adsorption-desorption isotherms of HC-x.

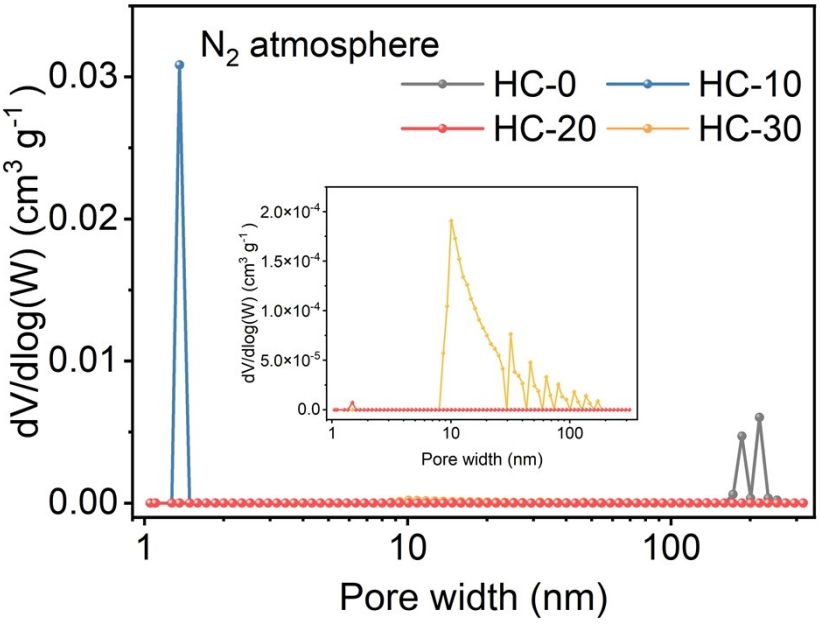

Fig. S5 Pore size distribution of HC-x at N_2 adsorption-desorption isotherms.

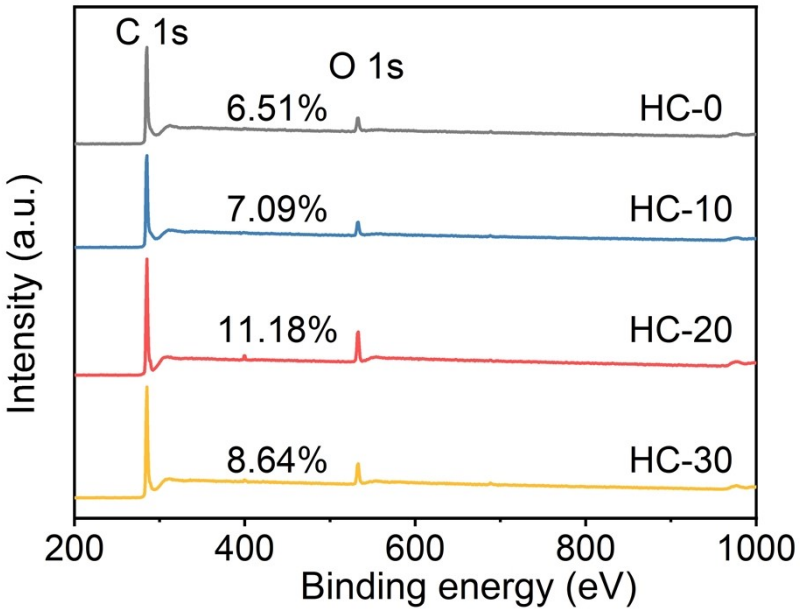

Fig. S6 XPS survey spectra of HC-0, HC-10, HC-20, and HC-30.

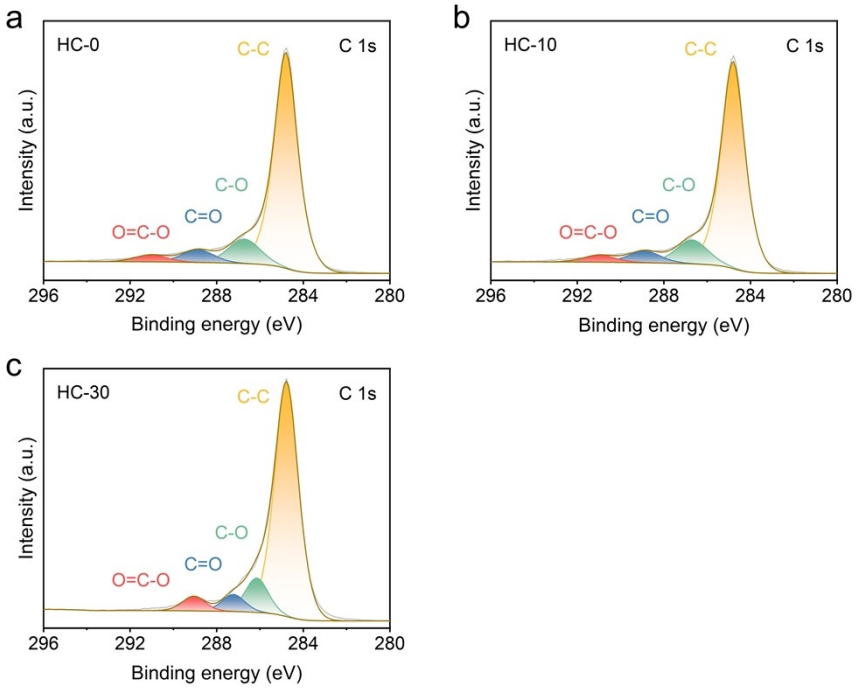

Fig. S7 High-resolution C 1s XPS spectra of (a) HC-0, (b) HC-10, and (c) HC-30.

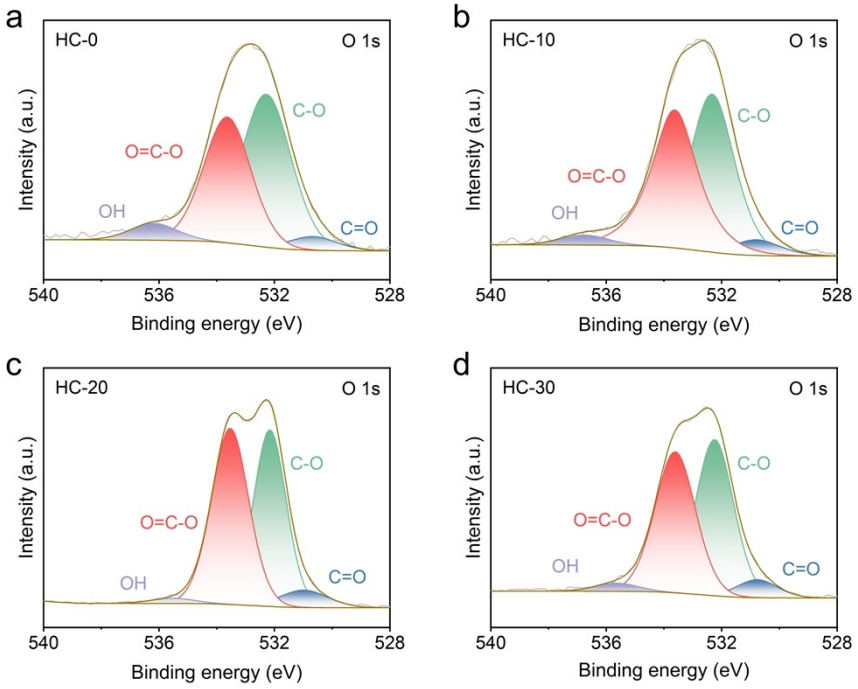

Fig. S8 High-resolution O 1s XPS spectra of (a) HC-0, (b) HC-10, (c) HC-20, and (d) HC-30.

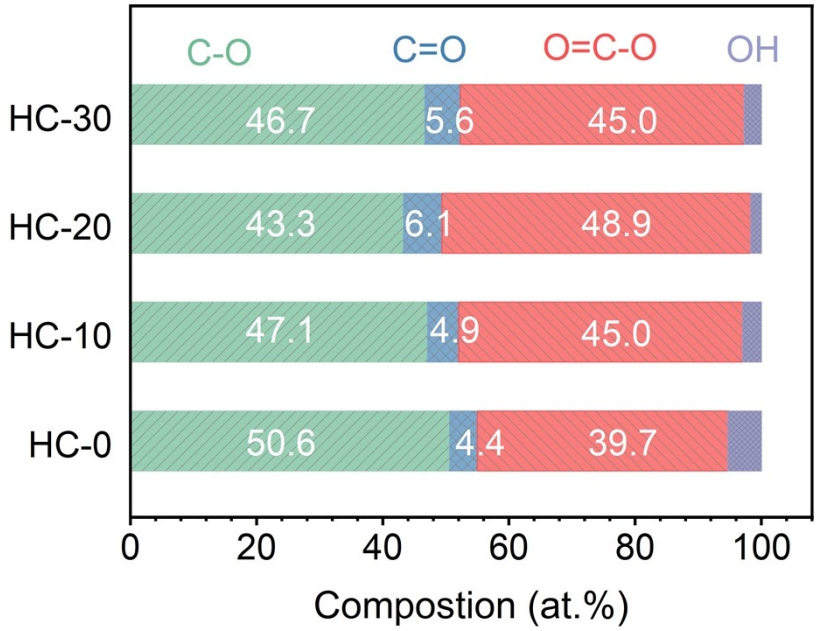

Fig. S9 Corresponding group contributions in HC-x of O1s XPS spectra.

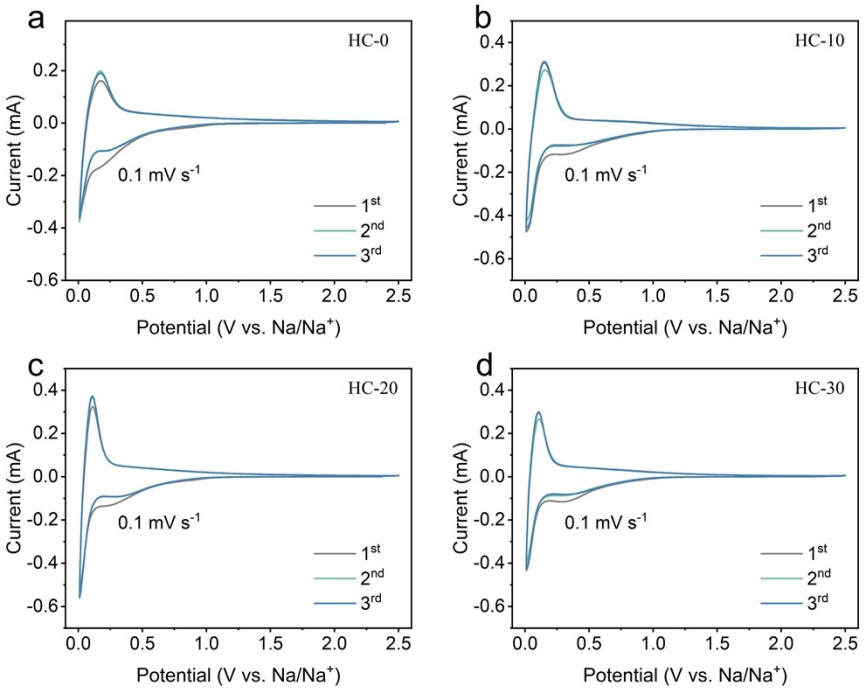

Fig. S10 CV curves of (a) HC-0, (b) HC-10, (c) HC-20, and (d) HC-30 anode at the scanning rate of 0.1 mV s^{-1}.

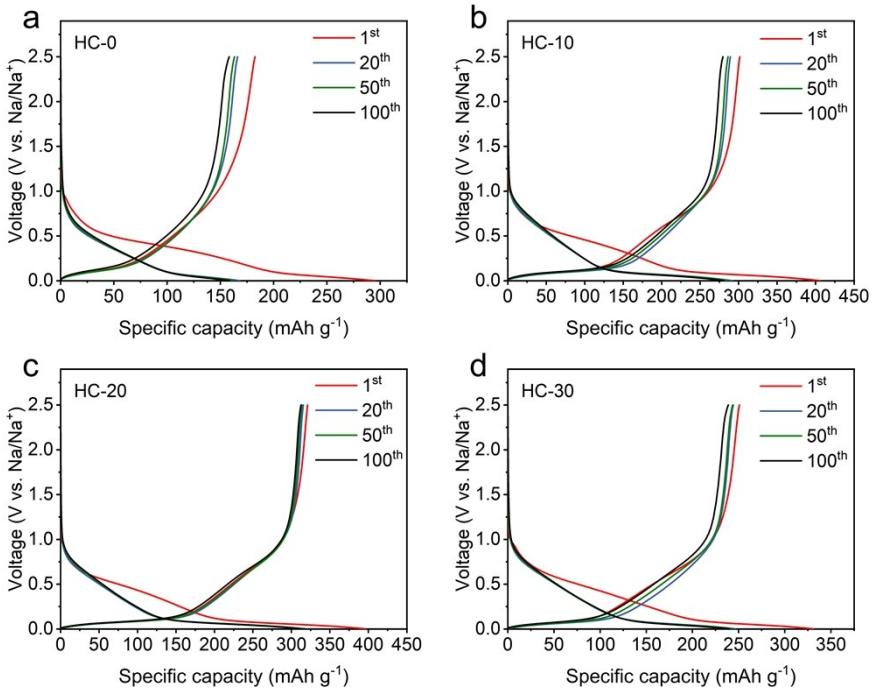

Fig. S11 GCD curves of (a) HC-0, (b) HC-10, (c) HC-20, and (d) HC-30 at 1st, 20th, 50th, and 100th cycles.

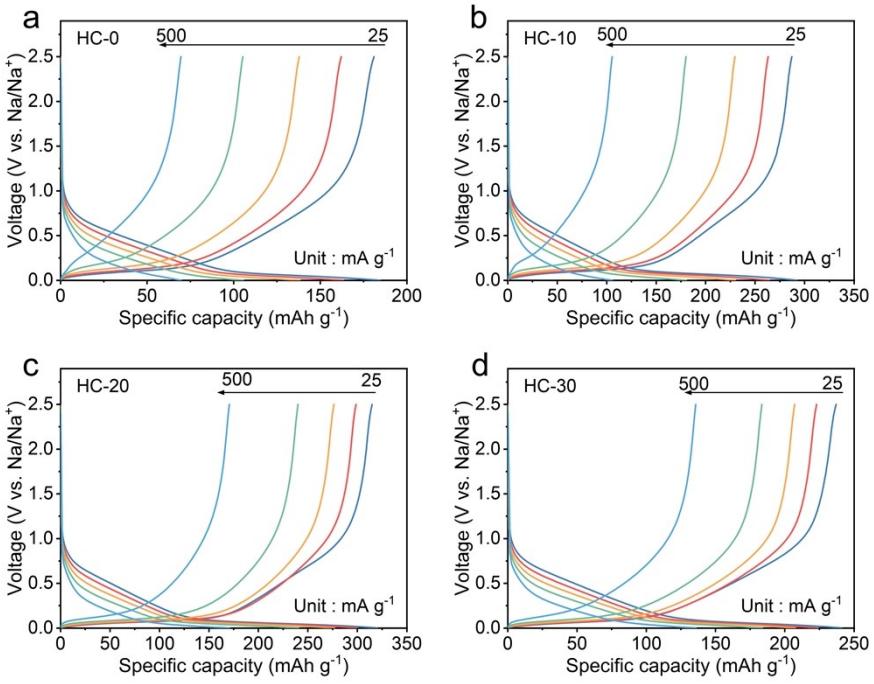

Fig. S12 GCD curves at different current densities of (a) HC-0, (b) HC-10, (c) HC-20, and (d) HC-30.

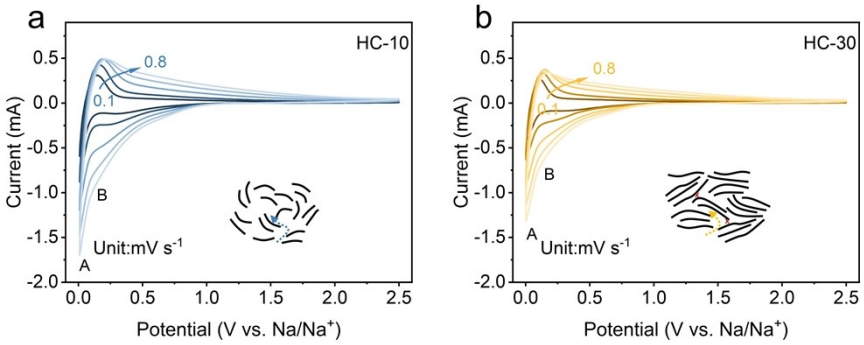

Fig. S13 CV curves of (a) HC-10 and (b) HC-30 at different scan rates.

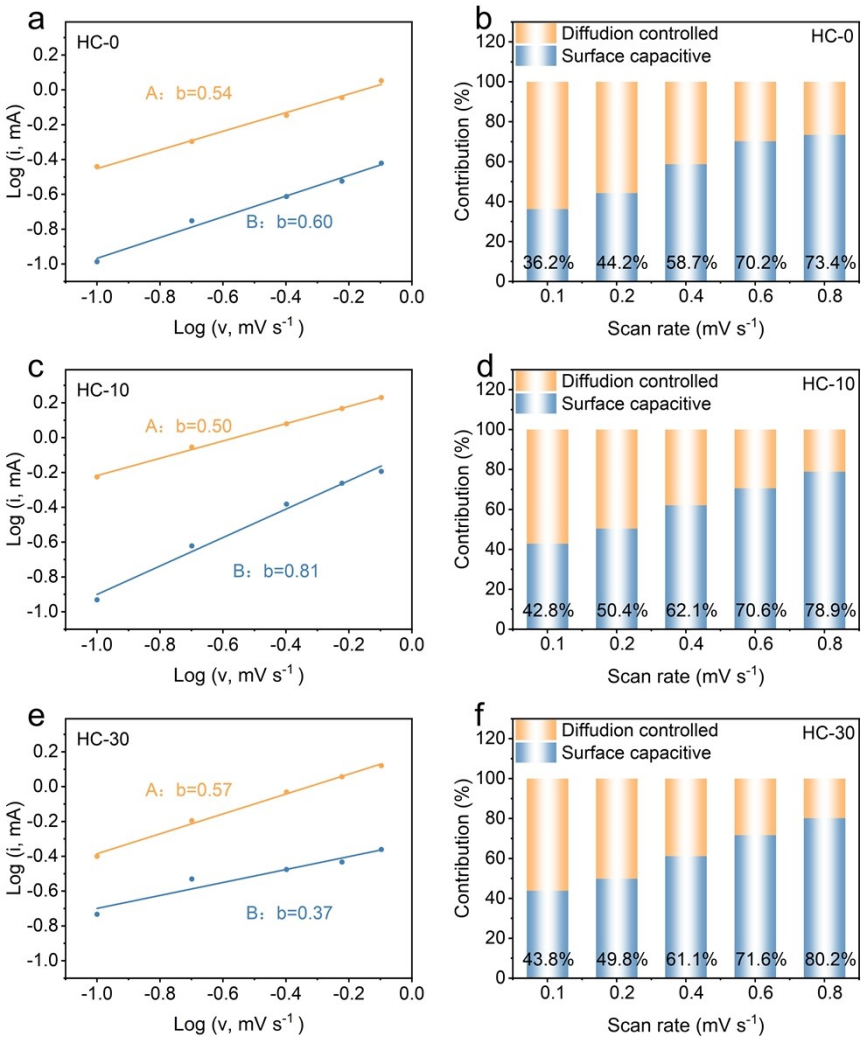

Fig. S14 b values of (a) HC-0, (c) HC-10, (e) HC-30. Contributions of the diffusion controlled and surface capacitive proportions in (b) HC-0, (d) HC-10, (f) HC-30 at various scanning rates.

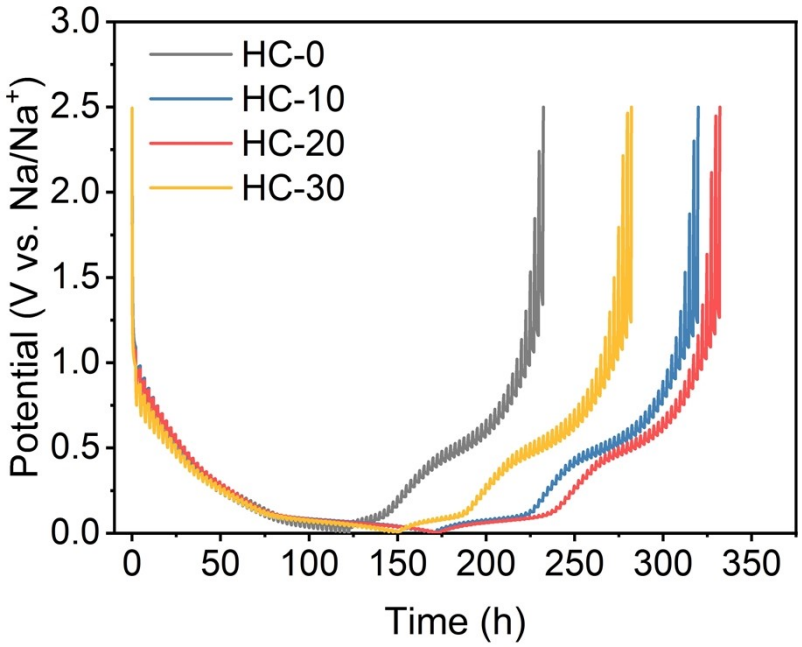

Fig. S15 GITT curves of HC-0, HC-10, HC-20, and HC-30.

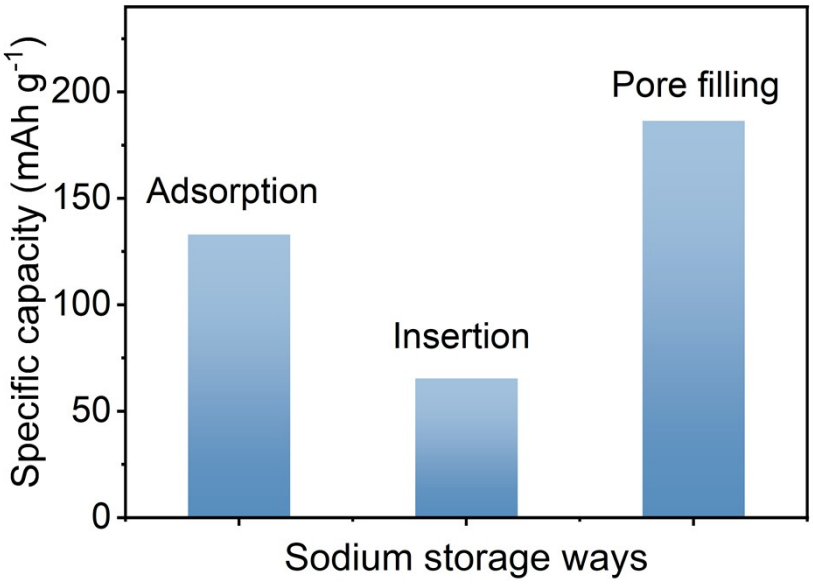

Fig.S16 Contribution of the sodium storage ways.

Table S1. The XRD characterizations of the samples.

Sample	2θ (°)	D_{002} (nm)	L_a	L_c
HC-0	21.3	0.417	3.21	0.86
HC-10	21.5	0.412	3.51	0.87
HC-20	23.3	0.381	3.53	0.88
HC-30	24.1	0.369	3.80	0.92

The calculation formula is as followed:[1,2]

$$d_{002}=\lambda/2\sin\theta_{002}$$

Where λ =0.154178 nm, $2\theta_{002}$ is the peak position of (002) peak in the XRD pattern.

$$L_a=1.84\lambda/B_{100}\cos\theta_{100}$$

$$L_c=0.89\lambda/B_{002}\cos\theta_{002}$$

Where λ =0.154178 nm, B_{100} and B_{002} are the full width at half maxima of the (100) and (002) peaks, the corresponding peak positions are θ_{100} and θ_{002}.

Table S2. Pore structure parameters of different samples from N_2 adsorption-desorption measurements.

Sample	S_{BET} (m^2 g^{-1})	$V_{open\ pores}$ (cm^3 g^{-1})
HC-0	39.80	0.01096
HC-10	10.60	0.00135
HC-20	2.13	0.00055
HC-30	1.35	0.00047

Table S3. The true density and the closed pore volume of the samples.

Sample	True density (g cm^{-3})	$V_{closed\ pore}$ (cm^3 g^{-1})
HC-0	1.832	0.103
HC-10	1.776	0.120
HC-20	1.703	0.145
HC-30	1.851	0.098

The calculation formula is as followed:

$$V_{closed\ pore}=\frac{1}{\rho_{true}}-\frac{1}{2.26}$$

Table S4. Fitting peak area proportion of C 1s and O 1s spectra in the XPS pattern of the different hard carbon materials.

sample	C 1s (%)				O 1s (%)			
	C=C	C-O	C=O	O=C-O	C=O	C-O	O=C-O	OH
HC-0	79.0	11.7	6.0	3.3	4.4	50.6	39.7	5.3
HC-10	78.9	11.8	5.8	3.5	4.9	47.1	45.0	3.0
HC-20	76.6	9.5	7.5	6.4	6.1	43.3	48.9	1.7
HC-30	78.9	11.0	5.4	4.7	5.6	46.7	45.0	2.7

Table S5. Comparison of the ICE and carbonization temperature of representative hard carbon anodes.

Sample	Carbonization temperature (℃)	ICE (%)
HCC6	1500	71.6
HC-C_{60}PF	1500	75.9
PCHC-10	1200	74.8
NPUCS	800	75.0
HHC	800	70.3
N/S-HC	1100	66.0
CNS-1300	1300	69.0
HCMS-3	1000	75.4
PHC-700	700	46.8
HC-9	1400	66.6
HC-0.2P-1000	1000	60.9

Table S6. Equivalent circuit fitting calculation results of EIS.

Sample	R_s (Ω)	R_{ct} (Ω)	σ (Ω $s^{-1/2}$)	D_{Na+} (cm^2 s^{-1})
HC-0	4.9	30.4	18.2	1.03E-16
HC-10	5.3	22.4	16.1	1.32E-16
HC-20	4.2	9.9	14.9	1.54E-16
HC-30	5.3	35.6	19.6	0.92E-16

The calculation formula is as followed:[3,4]

$$D=R^2T^2/2A^2n^4F^4C^2\sigma^2$$

Where R is the ideal gas constant, T is the absolute temperature, A refers to the surface area of the electrode, F is the Faraday constant, n is the transfer number of electrons per molecule during the reaction, C denotes the molar concentration of sodium ions, and σ is the slope of the $Z'\sim\omega^{-1/2}$ plot.

References

1 K. Wang, F. Sun, H. Wang, D. Wu, Y. Chao, J. Gao and G. Zhao, *Adv. Funct. Mater.*, 2022, **32**, 2203725.

2 Z. Zheng, S. Hu, W. Yin, J. Peng, R. Wang, J. Jin, B. He, Y. Gong, H. Wang and H. J. Fan, *Adv. Energy Mater.*, 2023, **14**, 2303064.

3 L. Zhong, X. Qiu, S. Hao, Z. Jiang and W. Zhang, *Chem. Eng. J.*, 2025, **516**, 164007.

4 B. Zhao, X. Li, L. Shang, C. Qiu, R. Yuan, H. Liu, T. Liu, A. Li, X. Chen and H. Song, *J. Mater. Chem. A*, 2024, **12**, 5834-5845.